Anomalous energy pathway of vacancy migration and self-diffusion in hcp Ti

S. L. Shang, L. G. Hector, Jr., Y. Wang, and Z. K. Liu

Phys. Rev. B **83**, 224104 — Published 17 June 2011

DOI: 10.1103/PhysRevB.83.224104

Anomalous Energy Pathway of Vacancy Migration and Self-Diffusion in hcp Ti

S. L. Shang,[1,*] L. G. Hector, Jr.,[2] Y. Wang,[1] and Z. K. Liu[1]

[1]*Department of Materials Science and Engineering, The Pennsylvania State University, University Park, Pennsylvania 16802*

[2]*Materials and Processes Laboratory, General Motors Research and Development Center, Warren, Michigan 48090*

An anomalous energy pathway with energetically-equivalent double saddle points for vacancy mediated self-diffusion within an hcp-Ti basal plane is unveiled by density functional theory. Examination of migration pathway and phonon force constants suggests that the migrating atom tries to follow the bcc-hcp phase transition via the Burgers shear deformation. We propose that the formed energy local minimum with a bcc-like atomic environment between the two saddle points originates from the existence of high-temperature bcc phase and is a feature of Group IV hcp metals with bcc-hcp phase transition. Computed diffusion coefficients are in favorable accord with experiments for hcp Ti.

PACS numbers: 66.30.Fq, 63.20.dk, 65.40.G-, 82.20.Db

I. INTRODUCTION

Diffusion is a thermally activated process that determines the properties of numerous materials. Recently, it has been demonstrated that quantitative prediction of diffusion coefficients in solid solutions as a function of temperature is possible via first-principles calculations within the framework of transition state theory.[1-10] During diffusion, a migrating atom passes through an energy barrier in moving from a local energy minimum site to another equivalent nearest neighbor site. The energy barrier or migration pathway is commonly thought to follow a bell-shaped profile with a "transition state" structure at its peak: this structure possesses a single imaginary frequency in its vibrational spectrum. Energy profiles that deviate from a bell-shaped profile have been noted commonly for diffusion involving interstitial sites,[7, 9, 10] and hence the bell-shaped profile is not universal. However, such behavior has not been noted for diffusion in most of the pure elemental solids such as fcc Al,[1] bcc Mo,[4] and hcp Mg.[6] The only observation of the flat shape or even the slightly double-peaked shape profile for vacancy migration was for hcp Zr by Verite *et al.*[11] from first-principles calculations. In the present work, we demonstrate that the migration pathway in the basal plane of hcp Ti possesses energetically-equivalent double saddle points, with a significantly reduced energy barrier for diffusion. We provide a simple physical picture for this observation.

Despite extensive research, fundamental diffusion properties of Ti are still far from fully understood. Of notable significance are the following: (i) there is a large difference (> 0.5 eV) in the vacancy formation energy in Ti from experiments[12-14] and first-principles predictions;[11, 15-17] (ii) self-diffusion coefficients and activation energies from measurements are scattered (see details later);[18-20] (iii) existing studies of vacancy migration are incomplete, and hence the

anomalous energy pathway for vacancy migration within a Ti basal plane with double saddle points, the subject of the present work, has not been reported.[11, 16] Numerous experimental difficulties render determination of diffusion properties in hcp materials challenging, with the most daunting issues being specimen purity, the availability of radioactive tracer elements, and large experimental uncertainties.[21] The present work is motivated by the fact that there are very few first-principles studies of diffusion in hcp metals. Notable examples are studies of self-diffusion in elemental Mg and Zn and impurity diffusion in Mg.[4-6] As for hcp-Ti, definitive first-principles calculations of self-diffusion are unavailable.[11, 16]

In this work, we employ first-principles density functional theory (DFT), the reaction rate theory of Erying,[22] transition state (or saddle point) structure search with the climbing image nudged elastic band (CI-NEB) method,[23] and the supercell (direct) method to lattice dynamics[24] to predict energy barriers for self-diffusion in hcp-Ti. Our focus on the energy barriers results from the fact that in addition to vacancy formation energies, they are a main contributor to self-diffusion coefficients perpendicular ($\perp$) and parallel to (//) the c-axis of hcp-Ti. Contrary to an existing study,[16] we find an anomalous energy pathway for vacancy migration within the basal plane of hcp-Ti with double saddle points. Our computed diffusion coefficients are found to be in close accord with experimental data.

II. COMPUTATIONAL METHODS

All calculations are based upon DFT as implemented in the Vienna Ab initio Simulation Package (VASP 5.2).[25] The ion-electron interaction was described by the projector augmented wave (PAW) method,[26] and the exchange-correlation part was treated within the PBEsol generalized gradient approximation (GGA) of Perdew-Burke-Ernzerhof (PBE).[27] The PBEsol functional has a

reduced gradient dependence:[28] this represents an improvement over the GGA in PW91 (Ref. 29) and PBE,[30] which frequently underestimate binding, elastic properties, and phonon frequencies, and frequently overestimate lattice parameters for most metals. Table I summarizes the predicted lattice parameters of hcp Ti using three potentials of PBEsol, PW91, and LDA (local density approximation)[31] in comparison with experiments.[32] Herein, the lattice parameters from PBEsol are in the middle of PW91 and LDA, while the results from PW91 are more close to experiments. Regarding the prediction of vacancy-mediated diffusion, we believe that the PBEsol is the best choice for hcp-Ti based on the present study and our previous investigations.[4-6] In the present work, the Ti potential treats the ten electrons in the s, d and filled-p levels as valence. For all calculations associated with the transition state searches, an 11×11×11 *k*-point mesh and 500 eV plane wave energy cutoff were adopted for the 3×3×2 supercells (36 atoms for the pure system and 35-atoms+1 vacancy for the vibrationally stable CI-NEB endpoint structures). Saddle point structures and associated minimum energy pathways were computed with the CI-NEB method.[23] Phonon spectra and related thermodynamic properties were computed with the supercell (direct) method to lattice dynamics.[24] During the VASP calculations, the Methfessel-Paxton smear method[33] was used in the relaxations and the calculations of forces acting on atoms. All VASP calculations were conducted within the MedeA computational environment,[34] with more details of first-principles, CI-NEB, and phonon calculations given in Refs. 5, 6.

III. RESULTS AND DISCUSSIONS

A. Energy pathway of vacancy migration

Figure 1 illustrates our predicted minimum energy pathways for vacancy migration within a basal plane (⊥ c-axis) and normal to a basal plane (// c-axis) for hcp-Ti using 5 images with the

CI-NEB method, where image 3 is located in the middle of the energy pathway for vacancy migration. For migration normal to a basal plane, image 3 is the saddle point structure, i.e. the transition state with a single imaginary frequency in the computed phonon spectra. However, migration within a basal plane is completely different. Here, an anomalous energy pathway, with energetically-equivalent double saddle points (images 2 and 4) and one local minimum (image 3) being 16 meV lower than the two, is predicted: this is in contrast to the common belief that a single saddle point exists in the middle of the vacancy-mediated energy pathway for elemental metals. A CI-NEB calculation with 7 images revealed the same behavior as that shown in Figure 1 with negligible energy differences (< 1 meV) with respect to the 5-image case. In addition, 5-image CI-NEB calculations using PW91-GGA and LDA potentials also predict the anomalous energy pathway in the basal plane. We can thus conclude that the anomalous energy pathway of vacancy migration in hcp-Ti is a fundamental result from DFT that is independent of the choice of exchange-correlation functional.

The origin of the anomalous energy pathway within a Ti basal plane may be understood in terms of the atomic positions of the migrating atom and the stretching force constants around the migrating atom. The positions 0 - 6 in Figure 2 correspond to the migrating atom in images 0 - 6 as shown in Figure 1, respectively. It is found that the migrating atom deviates from a straight line path between the starting (position 0) and ending (position 6) points with the maximum deviation being 0.23 Å at image 3. In fact, the migrating atom tries to follow the pathway of the bcc-hcp phase transition via the Burgers shear deformation,

Eq. 1 $(110)_{bcc}$ //$(0001)_{hcp}$ and $[\bar{1}11]_{bcc}$ //$[\bar{2}110]_{hcp}$

resulting in the relative movement of two neighboring basal planes along the 0-7 direction as shown in Figure 2: i.e., the movement of layer with filled symbols with respect to the layer with open symbols. However, the pathway of the Burgers deformation for the migrating Ti atom is hindered mainly by atom 8, the nearest neighbor of the migrating atom (in the same basal plane), due to electrostatic repulsion, and finally the migrating atom goes to the vacancy position 6, i.e., from 0, 1, …, to 6. In Figure 3, we inspect the local atomic environment around the migrating Ti atom. Here, the stretching force constants around the migrating Ti atom for images 0, 2, and 3 in Figure 1 based on phonon calculations are plotted. The force constants quantify the extent of interaction or bonding between the atoms. A large positive force constant suggests bonding, while a negative force constant suggests that the two atoms in question would 'prefer' to move apart.[35] In Figure 3, the examined region around the migrating Ti atom is constrained to the first nearest neighbor (NN) region based on the following definitions: (i) the bond length should be < ~ 3 Å since the NN distances are 2.8 ~ 2.9 Å for the 12 closed packed atoms in hcp-Ti (see Figure 3); (ii) the change of the NN bond length should be less apparent (e.g. < ~ 0.2 Å) at a bond length close to 3 Å, and (iii) the change of stretching force constant is also should be less apparent (e.g. < ~ 1 eV/Å^2) at a bond length close to 3 Å. Figure 3 shows that both the NN bond lengths and the stretching force constants are more scattered for images 2 and 3 within the basal plane than for images computed for the migration in a plane normal to the basal plane. For example, the NN bond lengths for image 3 are: 2.66 ~ 2.67 Å (// c-axis) vs. 2.56 ~ 2.92 Å (⊥ c-axis). Normal to the basal plane (// c-axis), the NN atoms around the migrating atom are 11, 4, and 4 for images 0, 2, and 3, respectively. While for the basal plane (⊥ c-axis), the NN atoms around the migrating atom are 11, 6, and 8 for images 0, 2, and 3, respectively. Therefore, the local minimum of image 3 for Ti migration in a basal plane (⊥ c-axis) has a bcc-like

environment with eight NN atoms. The scattered bond lengths (2.56 ~ 2.92 Å) and the scattered stretching force constants (0.35 ~ 2.44 eV/Å^2) of image 3 imply that the local bcc-like (migrating) Ti is heavily distorted: the formation of this bcc-like environment is likely derived from the stable high temperature bcc phase.[36]

Further examination of the average bond length change from images 0, 2, to 3 suggests that it decreases for Ti atom migration normal to a basal plane, but decreases and then increases for Ti atom migration within a basal plane: this is consistent with the two local minimum environments of images 0 and 3 within the basal plane. By checking the stretching force constants and the NN atoms around the migrating atom for hcp Mg and Zn,[6] we find that the 8-atom bcc-like environments are absent in middle of the vacancy-mediated energy pathways, and hence the normal energy pathways exist for self-diffusion both within and normal to a basal plane. In addition, more CI-NEB tests indicate that the similar anomalous energy pathways occur for hcp Zr and hcp-Hf within their basal planes as in the case of Ti and agreeing with the observation of hcp Zr by Verite *et al.*;[11] and the normal energy pathways with bell-shape profiles are presented for hcp-Sc and hcp-Tl within their basal planes, similar to the cases of hcp Mg and hcp Zn. It is proposed that the anomalous energy pathway existed at least in the Group IV metals of Ti, Zr, and Hf is due to the form of bcc-like environment with eight NN atoms possibly derived by the existence of the high temperature bcc phase.

B. Self-diffusion coefficients

One of the major applications of vacancy mediated energy barriers is the prediction of diffusion coefficients. This is especially critical since dominant diffusion mechanisms in alloys and

compounds are based on vacancy and interstitials with the former mostly for substitutional solutions and the latter for interstitial solutions. The self-diffusion coefficient for given direction d is,[37]

Eq. 2 $$D_d = f\langle d^2\rangle ZCw/2$$

where f is the jump correlation factor, $\langle d^2\rangle$ the component of the migration distance contributing to diffusion in the specific direction, Z the number of possible migration directions, C the vacancy concentration, and w the jump frequency. For hcp lattices, self-diffusion coefficients perpendicular ($D_\perp$) and parallel to ($D_{//}$) the c-axis are,[4, 6]

Eq. 3 $$D_\perp = \frac{1}{2}Ca^2(3f_{Ax}w_A + f_{Bx}w_B)$$

Eq. 4 $$D_{//} = \frac{3}{4}Cc^2 f_{Bz}w_B$$

where a and c are the hcp lattice parameters, w_A and w_B the jump frequencies perpendicular (jump A) and parallel (jump B) to the c-axis. f_{Ax}, f_{Bx} and f_{Bz} are the partial jump correlation factors for jumps A and B perpendicular (marked as x) and parallel (marked as z) to the c-axis, respectively, which are functions of the w_A/w_B ratio given by Mullen[38] graphically for hcp lattices. The vacancy concentration C can be calculated using a partition function according to the vacancy formation energy ΔG_f,

Eq. 5 $$C = \exp(-\Delta G_f / k_B T)$$

where $\Delta G_f = G_{IS} - ((N-1)/N)G_{PS}$ with G_{IS} and G_{PS} being the Gibbs energies for the initial state (*IS*) with one vacancy (i.e., image 0 in Figure 1), and the perfect state (*PS*) without a vacancy. The number of atoms in each supercell is N, T the temperature, and k_B Boltzman's constant. The jump frequency w of the migrating atom can be written according to Eyring's reaction rate theory as,[22]

Eq. 6 $$w = (k_B T / h)\exp(-\Delta G_m / k_B T)$$

where the vacancy migration energy $\Delta G_m = G_{TS} - G_{IS}$ with G_{TS} being the Gibbs energy for the transition state (*TS*) ignoring the contributions of imaginary vibrational frequencies to entropy and h Planck's constant. Here, G_{IS}, G_{PS}, and G_{TS} are obtained from first-principles and phonon calculations based on the harmonic approach[39] since quasiharmonic effects and thermal electronic contributions to thermodynamics on the diffusion properties are negligible.[1] Note that one of the energetically-equivalent saddle points within the basal plane (image 2, see Figure 1) is treated as the *TS*. Therefore, based on the first-principles CI-NEB and phonon calculations, the vacancy concentration (C) and the jump frequencies (w_A and w_B) can be predicted by Eq. 5 and and Eq. 6, respectively, and then the partial jump correlation factors (f_{Ax}, f_{Bx} and f_{Bz}) are resulted according to Mullen's graph.[38] Finally, the self-diffusion coefficients are obtained according to Eq. 3 and Eq. 4. More details to estimate first-principles self diffusion for hcp metals can be found in Ref. 6.

The aforementioned equations indicate that the diffusion coefficient is roughly inversely proportional to the exponential value of Gibbs energy of activation ($\Delta G_f + \Delta G_m$), i.e., diffusion coefficients follow the Arrhenius equation,

Eq. 7 $$D = D_0 \exp(-Q / k_B T)$$

where D_0 is a pre-exponential factor, Q the activation energy (enthalpy).

The relaxed vacancy formation energies ΔG_f's at 0 K (without the zero-point vibrational energies) are predicted to be 1.98 (PW91 GGA), 2.08 (LDA), and 2.14 eV (PBEsol). Ancillary calculations using a 72-atom supercell and PBEsol yields ΔG_f = 2.10 eV. The present ΔG_f's are

in close agreement with previous first-principles results (e.g., 2.14,[15] 2.13,[11] 2.08,[16] and 1.97 eV[17]), but larger than experiments (1.2,[12] 1.27,[14] and 1.55 eV [13]): this is due to the less pure specimens used in the experiments which significantly affect the diffusion properties of the "open" structure of hcp-Ti which possesses unusually large ionic-to-atomic radius ratio in comparison to "normal" hcp metals, such as Mg and Zn.[21] Regarding the vacancy migration energy, ΔG_m, the present predictions at 0 K are 0.40 eV ($\perp$ c-axis) and 0.52 eV (// c-axis) from PBEsol (see Figure 1) with the differences < 0.07 eV relative to predictions from PW91 GGA and LDA. We note that the present ΔG_m's are smaller than the Han *et al.*[16] first-principles value of 0.7 eV ($\perp$ c-axis): this may due to the small supercell (15 atoms with 1 vacancy) and the methodology of vacancy migration employed in their study. However, the present results are close to Verite's first-principles results,[11] see Table I for details.

Based on Eq. 3 and Eq. 4, Figure 4 shows the predicted Arrhenius diagram of self-diffusion coefficients perpendicular ($D_\perp$) and parallel ($D_{//}$) to the c-axis of hcp-Ti, together with experimental data from ultrapure[20] and the less pure[19] specimens. Our computed diffusion coefficients fall within the scatter of the experimental data suggesting excellent agreement with the trends indicated. The predicted pre-exponential factors $D_{0\perp}$ and $D_{0//}$ are 1.07×10^{-5} m^2/s and 1.20×10^{-5} m^2/s, respectively, with the present $D_{0\perp}$ greater than the measured $D_{0\perp}$ (1.07×10^{-8} m^2/s) from less pure specimens,[19] but less than the measured $D_{0\perp}$ (1.35×10^{-3} m^2/s) from ultrapure specimens.[20] Regarding activation energies, the present results are 2.57 eV ($Q_\perp$) and 2.65 eV ($Q_{//}$), while the measurements are scattered (1.27-2.39 eV,[18] 2.0 eV,[19] and 3.14 eV[20]): specimen purity is a likely cause. Similar to $D_{0\perp}$, the present $Q_\perp$ is larger than the measured $Q_\perp$ (2.0 eV) from less pure specimens,[19] but less than the measured $Q_\perp$ (3.14 eV) from ultrapure specimens.[20]

Note that both the measured $D_{0//}$ and $Q_{//}$ are absent. In addition, $D_{\perp}/D_{//} > 1$, as shown in Figure 4, primarily due to ΔG_m (//) > ΔG_m ($\perp$) (see Figure 1), agreeing with the general relation between c/a ratio and $D_{\perp}/D_{//}$ ratio for hcp metals, namely, $D_{\perp}/D_{//} > 1$ when $c/a < 1.633$, and vice versa.[20] Figure 4 shows that the present $D_{\perp}/D_{//}$ decreases from 3.0 to 2.0 with increasing temperature from 800 to 1155 K, in reasonable agreement with the measured value of 2.0 around 1000 K and the decreasing trend in $D_{\perp}/D_{//}$ values from ultrapure specimens.[20] For the sake of convenience, the diffusion-relative properties are also summarized in Table I.

IV. SUMMARY

In summary, the present first-principles CI-NEB calculations unveil an anomalous energy pathway containing energetically-equivalent double saddle points for vacancy migration within a basal plane of hcp-Ti. This is traceable from the Burgers shear deformation associated with the bcc-hcp phase transition based on the bcc-like atomic environment at the local energy minimum between the two saddle points. The driving force is likely the existence of bcc-Ti at high temperatures. It is also found that the anomalous energy pathways occur in Group IV elements of Ti, Zr, and Hf. Based on the predicted vacancy formation and migration energies from first-principles phonon calculations and Eyring's reaction rate theory, self-diffusion coefficients perpendicular and parallel to the c-axis of hcp-Ti were also predicted and found to be in close accord with experimental data.

ACKNOWLEDGMENTS

This work was funded by the National Science Foundation through Grant No. DMR-1006557, and we thank the GM Information Systems and Services for computational resources and technical support.

References and notes:

* Email: sus26@psu.edu

[1] M. Mantina, Y. Wang, R. Arroyave, L. Q. Chen, Z. K. Liu, and C. Wolverton, Phys. Rev. Lett. **100**, 215901 (2008).

[2] M. Mantina, Y. Wang, L. Q. Chen, Z. K. Liu, and C. Wolverton, Acta Mater. **57**, 4102 (2009).

[3] M. Mantina, S. L. Shang, Y. Wang, L. Q. Chen, and Z. K. Liu, Phys. Rev. B **80**, 184111 (2009).

[4] M. Mantina, L. Q. Chen, and Z. K. Liu, Defect Diff. Forum **294**, 1 (2009).

[5] S. Ganeshan, L. G. Hector Jr., and Z. K. Liu, Acta Mater. **59**, 3214 (2011).

[6] S. Ganeshan, L. G. Hector Jr., and Z. K. Liu, Comput. Mater. Sci **50**, 301 (2010).

[7] A. Van der Ven, J. C. Thomas, Q. C. Xu, B. Swoboda, and D. Morgan, Phys. Rev. B **78**, 104306 (2008).

[8] M. W. Ammann, J. P. Brodholt, J. Wookey, and D. P. Dobson, Nature **465**, 462 (2010).

[9] E. Wimmer, W. Wolf, J. Sticht, uuml, rgen, P. Saxe, C. B. Geller, R. Najafabadi, and G. A. Young, Phys. Rev. B **77**, 134305 (2008).

[10] S. C. Li, Z. Zhang, D. Sheppard, B. D. Kay, J. M. White, Y. Du, I. Lyubinetsky, G. Henkelman, and Z. Dohnalek, J. Am. Chem. Soc. **130**, 9080 (2008).

[11] G. Verite, F. Willaime, and C. C. Fu, Solid State Phenom. **129**, 75 (2007).

[12] I. I. Novikov, V. V. Roshchupkin, N. A. Semashko, and L. K. Fordeeva, J. Eng. Phys. Thermophys. **39**, 1316 (1981).

[13] V. O. Shestopal, Sov. Phys. Solid State **7**, 2798 (1966).

[14] E. Hashimoto, E. A. Smirnov, and T. Kino, J. Phys. F **14**, L215 (1984).

[15] O. Le Bacq, F. Willaime, and A. Pasturel, Phys. Rev. B **59**, 8508 (1999).

[16] X. L. Han, Q. Wang, D. L. Sun, and H. X. Zhang, Scr. Mater. **56**, 77 (2007).

[17] A. T. Raji, S. Scandolo, R. Mazzarello, S. Nsengiyumva, M. Harting, and D. T. Britton, Philos. Mag. **89**, 1629 (2009).

[18] J. Horvath, F. Dyment, and H. Mehrer, J. Nucl. Mater. **126**, 206 (1984).

[19] C. Herzig, R. Willecke, and K. Vieregge, Philos. Mag. A **63**, 949 (1991).

[20] M. Köppers, C. Herzig, and M. Friesel, Acta Mater. **45**, 4181 (1997).

[21] Y. Mishin and C. Herzig, Acta Mater. **48**, 589 (2000).

[22] H. Eyring, J. Chem. Phys. **3**, 107 (1935).

[23] G. Henkelman, B. P. Uberuaga, and H. Jonsson, J. Chem. Phys. **113**, 9901 (2000).

[24] K. Parlinski, Z. Q. Li, and Y. Kawazoe, Phys. Rev. Lett. **78**, 4063 (1997).

[25] G. Kresse and J. Furthmuller, Phys. Rev. B **54**, 11169 (1996).

[26] G. Kresse and D. Joubert, Phys. Rev. B **59**, 1758 (1999).

[27] J. P. Perdew, A. Ruzsinszky, G. Csonka, et al., Phys. Rev. Lett. **100**, 136406 (2008).

[28] J. P. Perdew and A. Zunger, Phys. Rev. B **23**, 5048 (1981).

[29] J. P. Perdew and Y. Wang, Phys. Rev. B **45**, 13244 (1992).

[30] J. P. Perdew, K. Burke, and M. Ernzerhof, Phys. Rev. Lett. **77**, 3865 (1996).

[31] D. M. Ceperley and B. J. Alder, Phys. Rev. Lett. **45**, 566 (1980).

[32] P. Villars and L. D. Calvert, *Pearson's handbook of crystallographic data for intermetallic phases* (ASTM International, Newbury, OH, 1991).

[33] M. Methfessel and A. T. Paxton, Phys. Rev. B **40**, 3616 (1989).

[34] MedeA 2.5, Materials Design Inc., Angel Fire, NM, USA (2009).

[35] S. L. Shang, L. G. Hector, Y. Wang, H. Zhang, and Z. K. Liu, J. Phys.-Condens. Matter **21**, 246001 (2009).
[36] E. Y. Tonkov and E. G. Ponyatovsky, *Phase transformations of elements under high pressure* (CRC Press, Boca Raton, Fla., 2005).
[37] N. L. Peterson, J. Nucl. Mater. **69-70**, 3 (1978).
[38] J. G. Mullen, Phys. Rev. **124**, 1723 (1961).
[39] S. L. Shang, Y. Wang, D. Kim, and Z. K. Liu, Comput. Mater. Sci **47**, 1040 (2010).

Tables

TABLE I. First-principles predictions and experimental results of hcp Ti, including equilibrium lattice parameters a_0 and c_0 (Å), mono-vacancy formation energy ΔG_f and migration energy ΔG_m (eV), pre-exponential factor D_0 (m^2/s), and activation energy Q (eV). ere, $\perp$ indicates the results perpendicular to c-axis, and // indicates the results parallel to c-axis.

Property	PW91[a]	LDA[a]	PBEsol[a]	Other works
a_0	2.932	2.863	2.899	2.951[b]
c_0	4.641	4.536	4.589	4.674[b]
ΔG_f	1.98[c]	2.08[c]	2.14[c]	1.97~2.14[e]
			2.10[d]	1.2~1.55[f]
ΔG_m ($\perp$)	0.44	0.33	0.40	0.7[g]
				0.43[h]
ΔG_m (//)	0.55	0.46	0.52	0.57[h]
$D_{0\perp}$			1.07×10^{-5}	1.07×10^{-8}[(i)]
				1.35×10^{-3}[(j)]
$D_{0//}$			1.20×10^{-5}	
$Q_\perp$			2.57	2.0[i]
				3.14[j]
				1.27-2.39[k]
				2.63[l]
$Q_{//}$			2.65	

[a] The present work predicted by different potentials
[b] Experimental data from Pearson's handbook.[32]
[c] Results based on 36-atom supercell.
[d] Results based on 72-atom supercell.
[e] Previous first-principles results of 2.14,[15] 2.13,[11] 2.08,[16] and 1.97.[17]
[f] Experimental data of 1.2,[12] 1.27,[14] and 1.55.[13]
[g] First-principles results.[16]
[h] First-principles results.[11]
[i] Measured results from less pure specimens.[19]
[j] Measured results from ultrapure specimens.[20]
[k] Average result measured from ploycrystal specimens.[18]
[l] Average result from first-principles results.[11]

Figures and Figure captions:

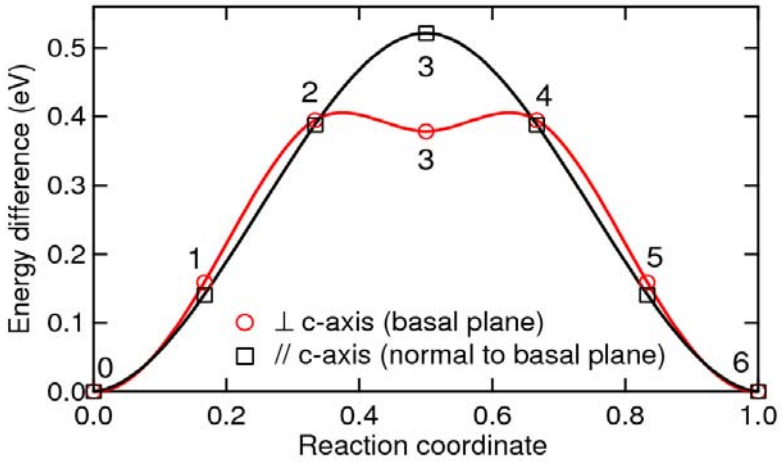

Figure 1. (Color online) Minimum energy pathways of hcp Ti within the basal plane (⊥ c-axis) and normal to the basal plane (// c-axis) predicted by first-principles CI-NEB method using 5 images.

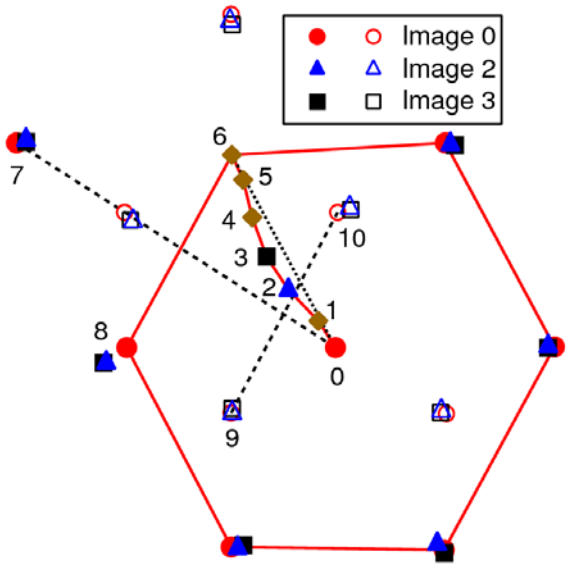

Figure 2. (Color online) Atomic positions for vacancy migration within a basal plane of hcp-Ti from first-principles CI-NEB calculations (view along the c-axis); the hexagonal structure with one vacancy (i.e., image 0) is indicated by the red lines. Positions 0 - 6 denote the migrating Ti atom in images 0 - 6 (see Figure 1), respectively. The filled symbols represent atoms in the basal plane, the open symbols denote atoms in a neighboring basal plane. For images 1, 4, 5, and 6, only the migrating Ti atom (filled diamond) is shown. The dashed line from 0-7 denotes the direction of relative movement between adjacent basal planes according to Burgers shear deformation for a bcc-hcp phase transition (movement from point 0 up to line 9-10). Atom 8 is the nearest neighbor (shown for images 0, 2 and 3 only) with respect to the migrating atoms 0 - 6, e.g., the bond lengths are 2.80 Å between 0-8, 2.60 Å between 2-8, and 2.56 Å between 3-8.

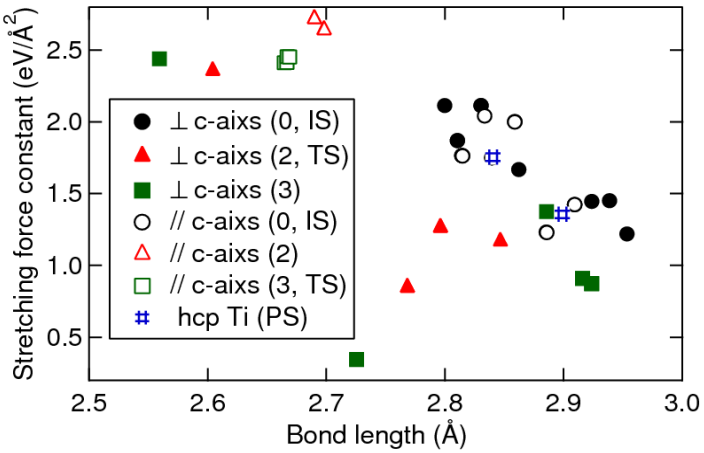

Figure 3. (Color online) Predicted stretching force constants around the migrating atom within the first nearest neighbor region (< ~ 3 Å, see text about the definition) for images 0 (*IS*), 2, and 3 (see Figure 1) and hcp Ti (*PS*). Note that *TS* indicates the transition state, 11 atoms exist for image 0 (both ⊥ and // c-axis), 4 for images 2 (// c-axis) and 3 (// c-axis), 6 for image 2 (⊥ c-axis), and 8 for image 3 (⊥ c-axis).

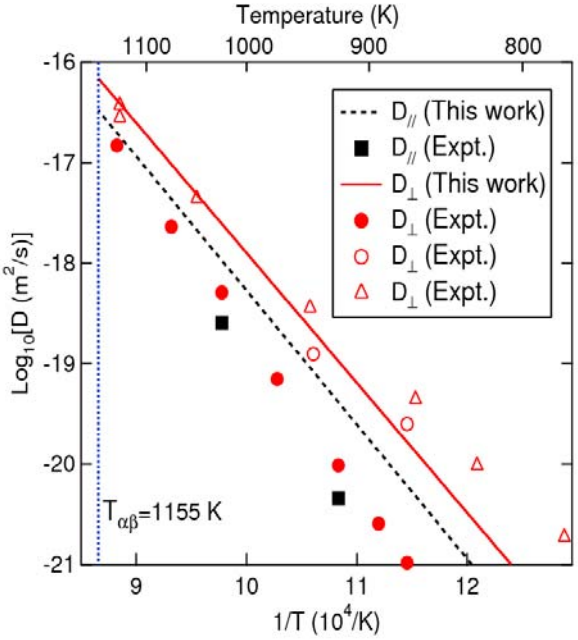

Figure 4. (Color online) Arrhenius diagram of self-diffusion coefficients perpendicular ($D_{\perp}$) and parallel ($D_{//}$) to c-axis of hcp Ti. The filled symbols are experimental data from ultrapure samples, and the open symbols from less pure samples. Open triangles are work of Herzig *et al.*,[19] other symbols are work of Köppers *et al.*,[20] and the vertical dotted line indicates the phase transition temperature of 1155 K between hcp α-Ti and bcc β-Ti.